Available online at www.sciencedirect.com
ScienceDirect
Journal of the European Ceramic Society 26 (2006) 3871–3879
www.elsevier.com/locate/jeurceramsoc

Hot corrosion and protection of Ti_2AlC against Na_2SO_4 salt in air

Zhijun Lin [a,b], Yanchun Zhou [a,*], Meishuan Li [a], Jingyang Wang [a]

[a] *Shenyang National Laboratory for Materials Science, Institute of Metal Research, Chinese Academy of Sciences, 72 Wenhua Road, Shenyang 110016, China*
[b] *Graduate School of Chinese Academy of Sciences, Beijing 100039, China*

Received 15 July 2005; received in revised form 30 October 2005; accepted 3 December 2005
Available online 18 January 2006

Abstract

The hot corrosion behavior of Na_2SO_4-coated Ti_2AlC was investigated by means of thermogravimetric analysis, X-ray diffraction, and scanning electron microscopy/energy dispersive spectroscopy. This carbide displays good hot corrosion resistance below the melting point of Na_2SO_4 while the corrosion attacks become virulent when the salt is molten. A protectively continuous Al_2O_3 layer forms and imparts good corrosion resistance, and consequently, the corrosion kinetics is generally parabolic at 850 °C. However, porous oxide scales fail to protect the Ti_2AlC substrate at 900 and 1000 °C. The segregation of sulfur at the corrosion scale/substrate interface accelerates the corrosion of Ti_2AlC. Furthermore, a convenient and efficient pre-oxidation method is proposed to improve the high-temperature hot corrosion resistance of Ti_2AlC. An Al_2O_3 scale formed during pre-oxidation treatment can remarkably restrain the infiltration of the molten salt into the substrate and prevent the substrate from severe corrosion attacks.

Keywords: Ti_2AlC; Al_2O_3; Corrosion

1. Introduction

Layered-ternary Ti_2AlC ceramic has attracted increasing interest in recent years due to its unique combination of the merits of both metals and ceramics,[1–13] such as, easy machinability, low density, good electrical and thermal conductivity, excellent thermal-shock and high-temperature-oxidation resistance. These salient properties make Ti_2AlC a highly promising candidate for high-temperature structural applications or as a coating material.

Jeitschko et al. deciphered the crystal information of Ti_2AlC in 1963.[1] It crystallizes in $P6_3/mmc$ symmetry and the crystal structure can be fundamentally described as strong Ti–C–Ti covalent-bonding chains being interleaved by closed-packed Al atomic planes. The electronic structure and bonding nature were reported.[2] Ti_2AlC is the most stable ternary-phase in the Ti–Al–C system.[3] Thereafter, a series of experimental and theoretical works have been reported on Ti_2AlC, including synthesis and mechanical properties of bulk material,[4–7] oxidation behavior,[8] theoretical predictions,[9] thin film deposition,[10] lattice dynamics,[11,12] and microstructural characterization.[13]

Poor oxidation resistance of TiAl and Ti_3Al intermetallics at elevated temperatures has been the bottleneck to their industrial applications.[14,15] It is interesting and surprising that, with relatively low aluminum content, a protectively continuous Al_2O_3 scale forms on the two ternary titanium–aluminum carbides in the Ti–Al–C system, i.e. Ti_3AlC_2 and Ti_2AlC substrate during high temperature oxidation in air.[8,16] The Al_2O_3 scale is adherent to the substrate and resistant to thermal cycling, which retards the further oxidation of these two carbides. Good high-temperature oxidation resistance and low density give Ti_2AlC the potential to be used in high-temperature oxidizing environments such as engine parts. In practical applications, ceramics may encounter various corrosive atmospheres. The hot corrosion attack of the salt-deposited samples would become serious and accelerate the degradation of materials under appropriate conditions.[17] It is therefore important to understand the effects of the deposited salt on the hot corrosion behavior of Ti_2AlC at high temperatures. Wang and Zhou[18] reported that the hot corrosion resistance of Ti_3AlC_2 was not satisfied at temperatures higher than 800 °C. However, information on the hot corrosion behavior of Ti_2AlC is sparse.

* Corresponding author. Tel.: +86 24 23971765; fax: +86 24 23891320.
E-mail address: yczhou@imr.ac.cn (Y. Zhou).

0955-2219/$ – see front matter © 2005 Elsevier Ltd. All rights reserved.
doi:10.1016/j.jeurceramsoc.2005.12.004

In this work, we investigated the hot corrosion behavior of the Na_2SO_4-coated Ti_2AlC in 850–1000 °C in air. The hot corrosion mechanism is discussed and an efficient pre-oxidation treatment is proposed to improve the high-temperature hot corrosion resistance of Ti_2AlC.

2. Experimental

2.1. Specimen preparation

Bulk polycrystalline Ti_2AlC ceramic was fabricated by a solid–liquid reaction and simultaneous in situ hot pressing method. Detailed descriptions on the synthesis of Ti_2AlC ceramic can be found elsewhere.[4] Specimens with dimensions of 10 mm in diameter and 2.5 mm in thickness were cut by electrical-discharge method. The as-cut specimens were ground down to 1500 grit SiC paper, polished to a 1 μm finish, and degreased in acetone. The pre-oxidation treatment was conducted in air at 1000 °C for 2 h. Both the pre-oxidized and untreated specimens were placed on a hot plate working at 200 °C; a salt film was then coated on the sample surface by brushing a saturated Na_2SO_4 solution. The amount of the salt was controlled to be $4.0 \pm 0.2\ mg/cm^2$.

2.2. Specimen characterizations

The hot corrosion tests were carried out in a Setsys 16/18 thermoanalyzer (Setaram, France). The continuous weight-changes during the experimental process were recorded using thermogravimetric analysis (TGA) with an accuracy of $\pm 4 \times 10^{-7}$ g. Specimens for TGA tests were suspended with a Pt wire and heated to the test temperatures at a rate of 40 °C/min. Duplicate runs were carried out to check the reproduction of tests. After the TGA test, the corroded samples were rinsed with hot water to remove the soluble salts. Thereafter, the phase components were identified by a step-scanning X-ray diffractometer with Cu Kα radiation (Rigaku D/max-2400, Japan). Both the surface and cross-sectional morphologies of the samples were observed by a S-360 scanning electron microscope (SEM) (Cambridge Instruments Ltd., UK) equipped with energy dispersive spectroscopy (EDS). Prior to SEM observations, a thin gold layer was sputtered on the hot corroded specimens to ensure good electrical conductivity.

3. Results and discussions

3.1. Corrosion kinetics

Duplicate runs show that the corrosion kinetics is reproducible with deviations within 5%. The weight-changes/area versus time of Na_2SO_4-coated Ti_2AlC in air at 850–1000 °C is presented in Fig. 1. At temperatures above the melting point of Na_2SO_4 (884 °C), where Na_2SO_4 is present in molten form, the hot corrosion kinetics shows a typical tri-stage characteristic as shown in the inset (a) of Fig. 1. On the other hand, the weight-changes are relatively low and generally obey a parabolic rate law at 850 °C, which can be seen in the inset (b) of Fig. 1.

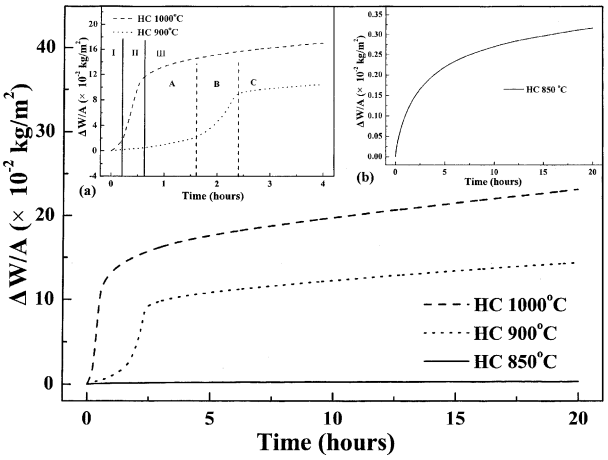

Fig. 1. Weight-changes pre unit area vs. time of Na_2SO_4-coated Ti_2AlC corroded in air at 850–1000 °C for 20 h. Enlarged view in the inset (a) displays typical tri-stage corrosion characteristics. 'I/A', 'II/B', and 'III/C' indicate the first, second, and third corrosion stages, respectively. Inset (b) shows the parabolic weight-change feature of Ti_2AlC corroded at 850 °C. 'HC' denotes 'hot corrosion'.

Similar tri-stage characteristic was observed in the hot corrosion of Ti_3AlC_2 at 900 °C.[18] At the first stage, the so-called gestation/or incubation period, the weight-changes increase at relatively slow rates, i.e. 1.2 and 8.0 mg cm^{-2} h^{-1} at 900 and 1000 °C, respectively. At the second stage, the so-called high-speed corrosion stage, weight-changes increase remarkably. For example, the weight-change rates are 8.4 and 27 mg cm^{-2} h^{-1} at 900 and 1000 °C, respectively. After this high-speed corrosion stage, thick oxide scales formed on the Ti_2AlC substrate and the corrosion reached a relatively steady stage, wherein the hot corrosion rates are low (less than 0.50 mg cm^{-2} h^{-1}). The second stage is characterized by a high-speed weight-change rate. The high-speed corrosion consumes a lot of salt and the salt decreases rapidly. Consequently, the weight-change rates are much lower at the third stage.

We compare the corrosion kinetics of two ternary carbides, Ti_2AlC and Ti_3AlC_2, to understand the influence of chemical composition on the corrosion resistance. The hot corrosion kinetics of Ti_3AlC_2 displays a tri-stage characteristic at 900 °C,[18] which is similar to those of Ti_2AlC. However, the linear weight-change rates of Ti_3AlC_2 are much higher than those of Ti_2AlC. In addition, the corrosion kinetics of Ti_3AlC_2 is linear at 800 °C while the kinetics is parabolic for Ti_2AlC up to 850 °C. In a word, Ti_2AlC displays higher corrosion-resistance against Na_2SO_4 salt than Ti_3AlC_2. The corrosion kinetics of Ti_2AlC will be further discussed in the following sections.

3.2. Determination of crystalline phases in the hot corroded samples

XRD analysis reveals that the as-synthesized specimen is single-phase Ti_2AlC (Fig. 2a). Corrosion products were determined by XRD after the TGA test and the results are displayed in Fig. 2b–d. For the sample corroded at 850 °C, the dominant phase is Ti_2AlC, suggesting that the corrosion scale is thin. However, the reflections of Ti_2AlC could hardly be detected

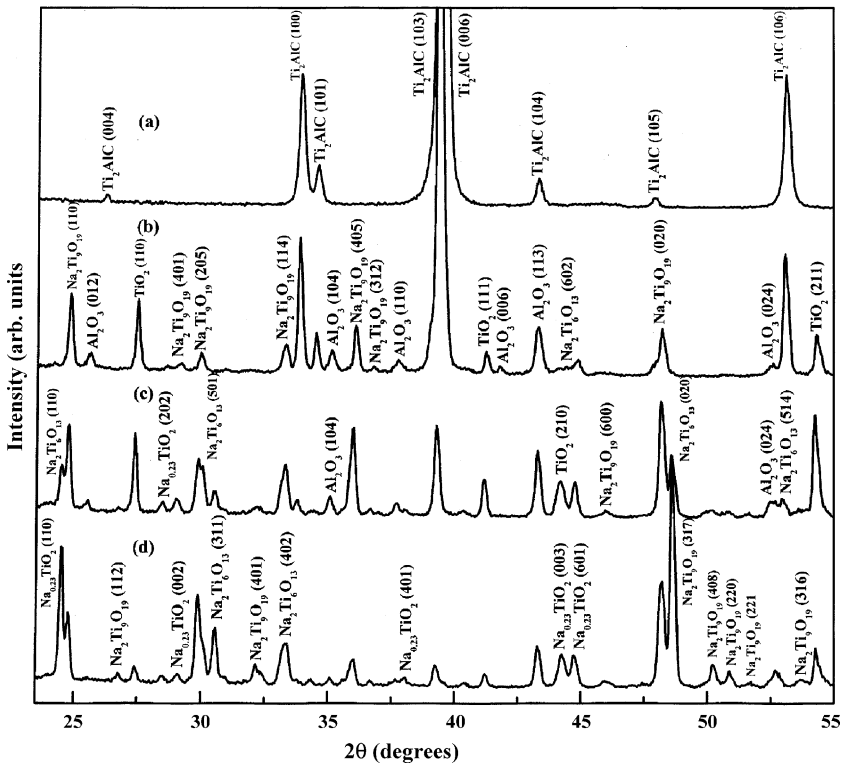

Fig. 2. XRD patterns of four Ti_2AlC specimens. (a) Untreated; (b)–(d) are samples after hot corrosion for 20 h at 850, 900, and 1000 °C, respectively.

by XRD on the samples hot corroded at 900 and 1000 °C, which indicates that the corrosion scales are too thick for the substrate to be detected. At 850–1000 °C, Na-containing species, such as $Na_{0.23}TiO_2$, $Na_2Ti_9O_{19}$ ($Na_2O{\cdot}9TiO_2$), and $Na_2Ti_6O_{13}$ ($Na_2O{\cdot}6TiO_2$) were detected; and the intensities increase with temperatures. Mobin and Malik[19] studied the interaction of TiO_2 and Na_2SO_4 at 823–923 °C and revealed that the interaction would lead to sodium–titanium oxides formation. It is reasonable that the presence of Na–Ti oxides can be attributed to the reaction between Na_2SO_4 and TiO_2. Few sodium aluminum oxides were detected because the corrosion of Al_2O_3 at this temperature range is small.[20]

3.3. Surface microstructure of the hot corroded samples

Surface morphologies of Na_2SO_4-coated Ti_2AlC hot corroded in air at 850–1000 °C for 20 h display different characteristics. As can be seen in Fig. 3a, the surface of the sample corroded at 850 °C is relatively smooth, suggesting that the interaction between surface oxides and the salt is slight. Some corrosion products remained on the sample surface and they were determined to contain mainly Ti, O, and Na by EDS compositional analysis. Surface morphologies of specimens hot corroded at 900 and 1000 °C show sharp difference. Typical surface morphology of the sample hot corroded at 900 °C is shown in Fig. 3b. Obviously, Ti_2AlC suffers severe attacks by the molten salt. It is noted that most of corrosion products at 900 °C are needle-shape. EDS analysis reveals that the products contain mainly Ti, Al, Na, and O elements. Combining the XRD results (Fig. 2c), the acicular products are mixtures of Al_2O_3 and sodium titanium oxides. Fig. 3c is the surface morphology of the sample corroded at 1000 °C; enlarged view of the globular appearance is shown in the inset. The surface of the specimen hot corroded at 1000 °C is uneven and non-uniform. Globular products are popular besides the acicular products similar to those at 900 °C. Compositional analysis by EDS indicated that the globular products mainly consist of Ti and O plus a minor amount of Na and Al.

Micropores are present on the surfaces of the samples hot corroded at 900 and 1000 °C (Fig. 3b–c), which can be attributed to the expulsion of gas species during hot corrosion. Berthold and Nickel[21] systematically investigated the hot corrosion behavior of silica and silica-formers and reported that silicon nitride and carbide could act as effective reduction agents. Thermodynamic calculations show that Na_2SO_4 is not stable under reducing conditions and leads to the formation of Na_2S according to:[21]

$$Na_2SO_4 \Leftrightarrow Na_2S + 2O_2 \quad (1)$$

The formation of Na_2S may also favor the following reaction:[21]

$$3Na_2SO_4 + Na_2S \Rightarrow 4Na_2O + 4SO_2 \quad (2)$$

Similarly, Ti_2AlC can act as a reduction agent. As a consequence, the expulsion of gas species left micropores on the surface.

3.4. Cross-sectional analysis of the corrosion scales

Cross-sectional analysis can provide fundamental information on the corrosion process and is important to understand

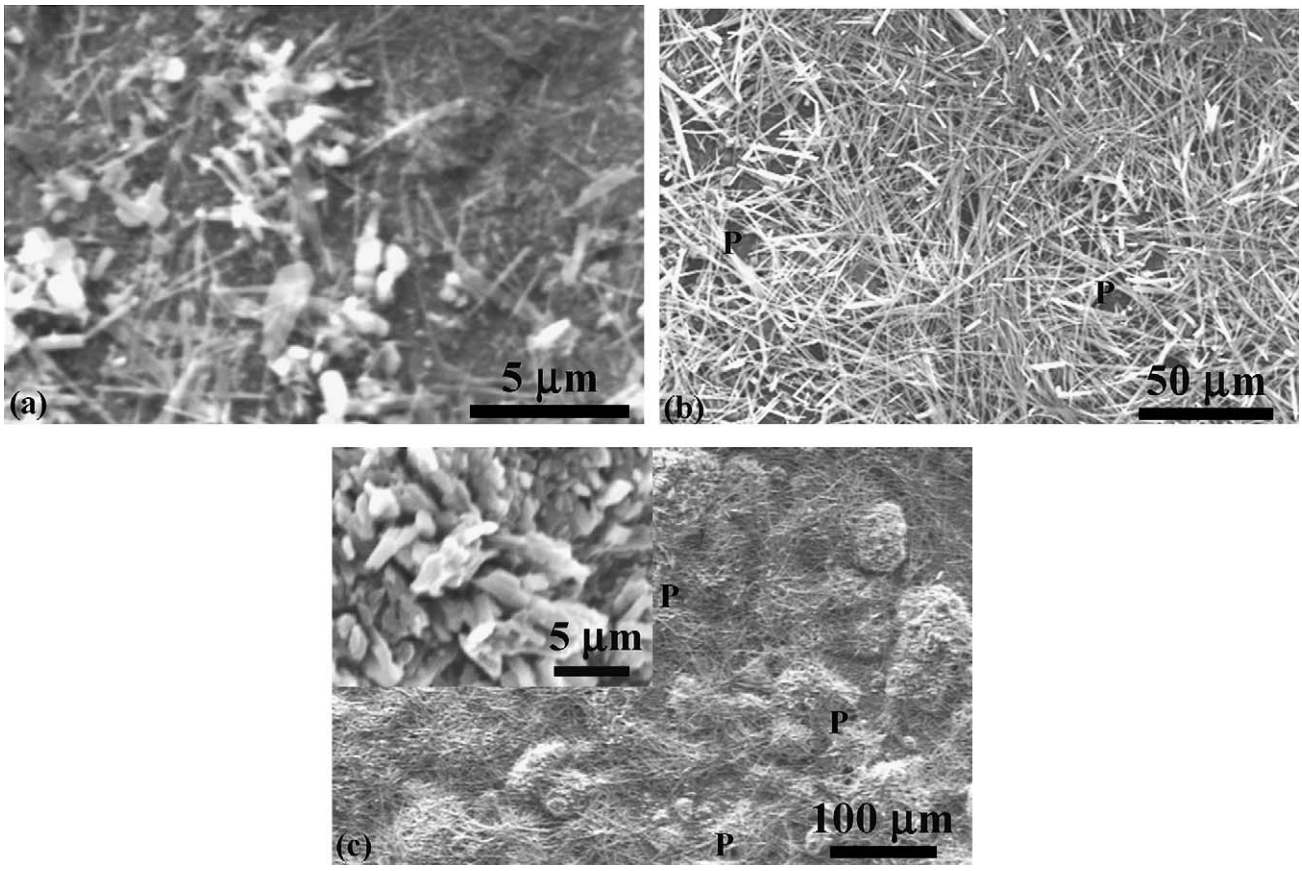

Fig. 3. Surface morphologies of Ti_2AlC corroded at: (a) 850 °C; (b) 900 °C; and (c) 1000 °C for 20 h. 'P' indicates 'pore'.

the nature of attack on the Ti_2AlC substrate. Hence, the cross-sectional microstructures of the samples after hot corrosion were also investigated.

Fig. 4a shows the backscattered electron image of the cross-section of Na_2SO_4-coated Ti_2AlC after hot corrosion at 850 °C for 20 h. The corrosion scale is approximately 4 μm in thickness and a continuous Al_2O_3 scale is present; the Al_2O_3 scale is further confirmed by the EDS line-scanning result shown in Fig. 5a. It is clear that a protective Al_2O_3 scale formed and thus further corrosion was controlled by the diffusion through the Al_2O_3 scale. Consequently, the hot corrosion kinetics is parabolic (Fig. 1). Cross-sectional views of the specimens hot corroded at 900 and 1000 °C are also displayed in Fig. 4b–c. EDS analysis indicates that the dark-gray regions in the corrosion scales are rich in Al_2O_3 while the light-gray regions are rich in TiO_2. No continuous Al_2O_3 scale formed in both samples and Al_2O_3 tends to locate at the outer scale. The thickness of the scales increases markedly with temperature (approximately 260 and 430 μm, at 900 and 1000 °C, respectively), revealing that Ti_2AlC suffered severe attacks by Na_2SO_4 at high temperatures, which agrees well with the high weight-change rates (Fig. 1). Pores are also obvious in the cross-sections; some small pores even extend to the forefront of the subsurface and accelerate the degradation of the substrate.

Compositional line-scanning along the lines shown in Fig. 4b–c are displayed in Fig. 5b–c. The most distinguished feature is that sulfur-rich area is present at the scale/Ti_2AlC substrate interface for the specimens hot corroded at 900 and 1000 °C. The segregation of sulfur was also observed during the hot corrosion of Ti_3AlC_2.[18] The presence of sulfur-rich bands at the substrate/scale interfaces demonstrates that chemical reaction of Ti_2AlC with Na_2SO_4 occurred during hot corrosion.

3.5. Corrosion mechanism of Na_2SO_4-coated Ti_2AlC

A protectively continuous Al_2O_3 layer forms during high-temperature oxidation in air and results in good oxidation resistance.[8] Similarly, the cross-sectional analysis on the specimen corroded at 850 °C reveals that a protective Al_2O_3 scale forms during the hot corrosion of Ti_2AlC. The Al_2O_3 scale retarded the hot corrosion of the substrate and the hot corrosion process was controlled by the diffusion through the Al_2O_3 scale. Consequently, the weight-change rates are low at 850 °C. Unlike oxidation of salt-free samples in air, no continuous Al_2O_3 layer was observed after hot corrosion at 900 and 1000 °C. The difference lies in the presence of a Na_2SO_4 film. Therefore, the effect of Na_2SO_4 should be discussed.

The acid–basic nature of Na_2SO_4 can be described as:[22]

$$Na_2SO_4 = Na_2O + SO_3 \quad (3)$$

where SO_3 is an acidic component while Na_2O is a basic one. The consumption of either SO_3 or Na_2O will favor the dissoci-

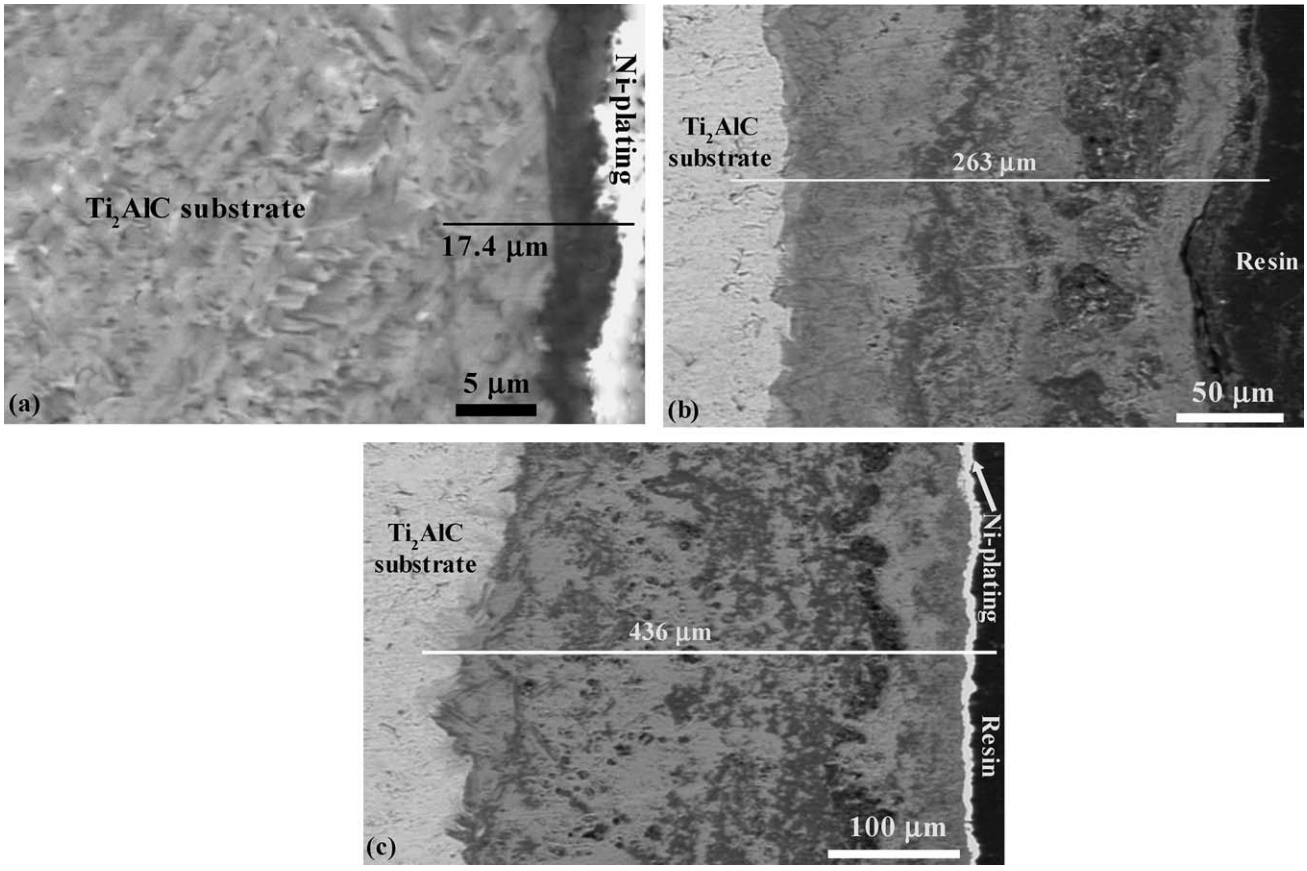

Fig. 4. SEM backscattered electron images of the cross-sections of Ti_2AlC after hot corrosion for 20 h at: (a) 850 °C; (b) 900 °C; and (c) 1000 °C, respectively.

ation of Na_2SO_4. SO_3 has the equilibrium:

$$SO_3 = SO_2 + \tfrac{1}{2}O_2 \quad (4)$$

A thin oxide scale will form during the heating to the test temperatures. The following reaction is presumably to take place first:

$$4Ti_2AlC + 13O_2 = 8TiO_2 + 2Al_2O_3 + 4CO \quad (5)$$

At 850 °C, sodium sulfide is in solid state and the activity of Na_2O is relatively low. Therefore, the preformed thin oxide scale can protect the substrate. As the corrosion persists, the oxide scale grew thicker and further corrosion was controlled by the diffusion through the scale. Consequently, the corrosion behavior is similar to the oxidation in air. The hot corrosion occurred by the interaction of TiO_2 and the salt. The oxidation of Ti_2AlC consumes oxygen as described by Eq. (5) and favors the decomposition of SO_3. The consump-

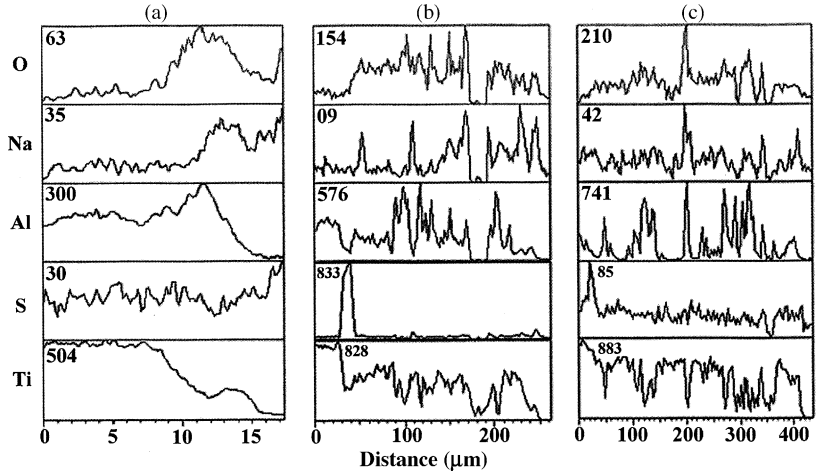

Fig. 5. (a)–(c) EDS line-scanning results along the lines shown in Fig. 4a–c, respectively. It is obvious that sulfur-rich bands are present at the corrosion scale/substrate interface at 900 and 1000 °C.

tion of SO_3 according to Eq. (4) promotes the dissociation of Na_2SO_4. As a result, the activity of Na_2O increases; the Na_2O reacts with TiO_2 and leads to the formation of sodium–titanium oxides.

The increase of basicity in molten salt also promotes the basic dissolution of oxides especially Al_2O_3 according to the following equation:

$$Al_2O_3 + Na_2O = 2NaAlO_2 \quad (6)$$

After basic dissolution of Al_2O_3 occurs, the AlO_2^- ions will migrate to the regions with lower basicity. In the place where Al_2O_3 can stably exist, it precipitated again,[18] that is why the outer scales are rich in Al_2O_3.

At temperatures above the melting point of sodium sulfide, Na_2SO_4 is in molten state and the corrosion attacks become virulent. In this circumstance, the molten salt can easily penetrate to the substrate and prevent the formation of a continuously protective oxide scale. As a result, the chemical reactions between Ti_2AlC and the Na_2SO_4 salt dominate the corrosion process and sulfur segregates at the corrosion scales/Ti_2AlC substrate interface. As the corrosion persists, the corrosion scales become thicker and the expulsion of gases species left pores on the scales. The porous and non-protective scales fail to protect the Ti_2AlC substrate and the corrosion kinetics is generally linear.

The corrosion kinetics at 850 °C is parabolic and continuous Al_2O_3 scale is present; it is plausible that diffusion of ions determines the corrosion rate in this temperature. The corrosion scales at 900 and 1000 °C are porous and the corrosion kinetics is generally linear. Therefore, the rate-limiting step is the chemical reactions between the molten salt and Ti_2AlC.

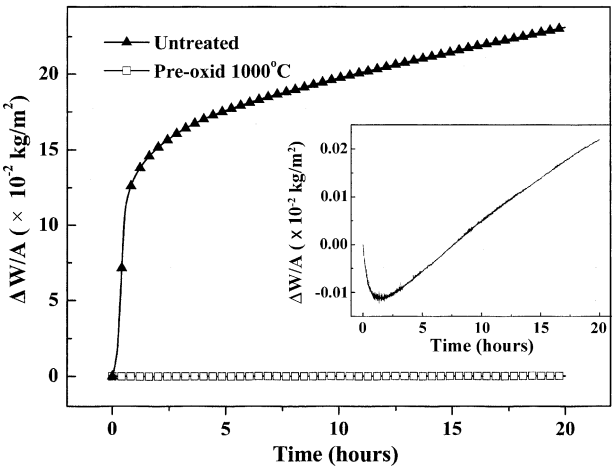

Fig. 6. Weight-changes/area vs. time of pre-oxidized and untreated samples hot corroded at 1000 °C for 20 h. Enlarged view of the pre-oxidized specimen is plotted in the inset.

3.6. Improving the hot corrosion resistance by pre-oxidation

Since Ti_2AlC suffers serious hot corrosion at 900 and 1000 °C, it is necessary to protect this technically important ceramic. Alternatively, alloying additions and surface modification are two widely applied ways to improve the corrosion resistance of alloys.[23] But alloying additions always deteriorates the mechanical properties of the substrate. Pre-oxidation has been proved to be a highly efficient and convenient surface modification method. For example, Lang et al.[24] improved the oxidation resistance of Fe–40Al sheet by pre-oxidation in air at 1100 °C. The pre-oxidation treatment in this work was inspired

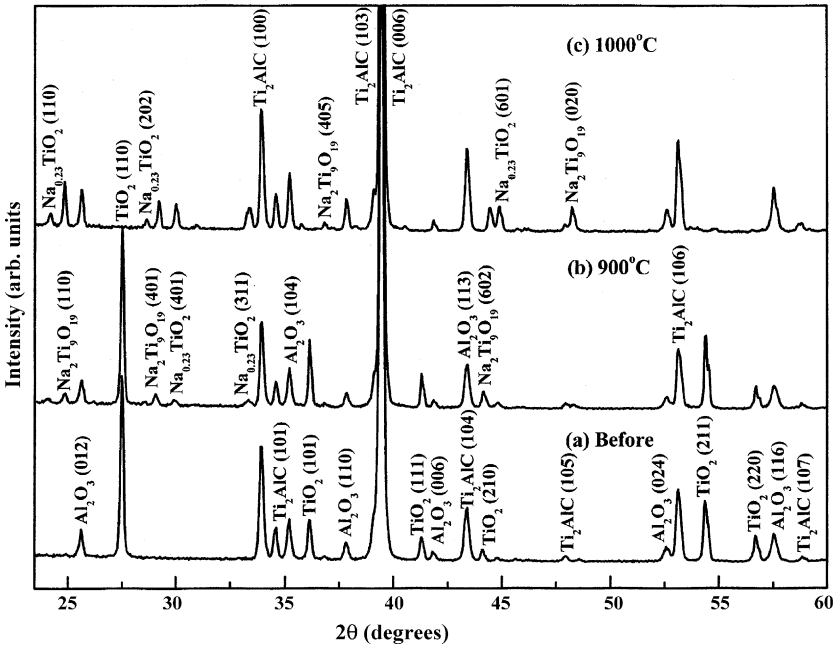

Fig. 7. XRD patterns of the three pre-oxidized samples (a) before; (b) and (c) after hot corrosion for 20 h at 900 and 1000 °C, respectively.

by the fact that a continuously protective Al_2O_3 scale forms on Ti_2AlC substrate during high-temperature oxidation in air.

Pre-oxidation treatment was conducted in air at 1000 °C for 2 h. The pre-oxidized specimens were then coated with the same amount of salt and exposed to the same environments as the untreated samples.

Fig. 6 shows the weight-changes/area versus time of pre-oxidized and untreated samples hot corroded at 1000 °C. Weight-changes of the sample corroded at 900 °C show similar characteristics and are not shown for briefness. Enlarged view of the kinetics curve of the pre-oxidized sample is plotted in the inset. The final weight-changes of the pre-oxidized samples are much lower than the untreated samples, indicating that pre-oxidation treatment remarkably inhibits the corrosion.

It is noted that a rapid weight-loss occurred in the initial stage, which is similar to the interaction of TiC powders with Na_2SO_4 reported by Mobin and Malik.[25] The initial rapid weight-loss is presumably due to the expulsion of gases species. The final weight-change of the pre-oxidized specimen is four orders of magnitude lower than the untreated sample. This result is consistent with the work reported by Lawson et al.,[20] in which they systematically investigated the hot corrosion behavior of Al_2O_3 at 700 and 1000 °C under different atmospheres and revealed that the corrosion attacks were small and brought little weight-changes.

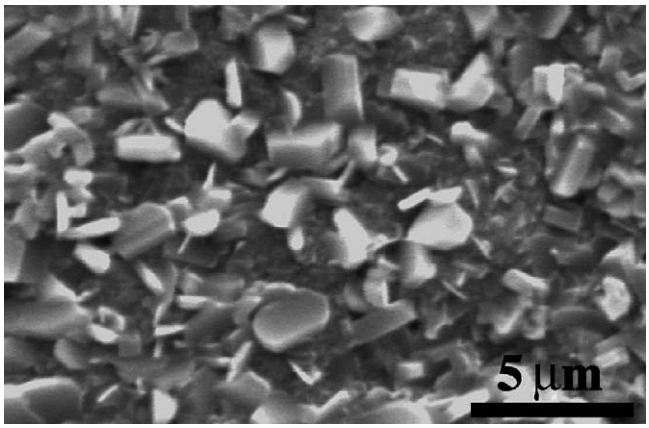

Fig. 8. Surface morphology of the pre-oxidized sample after hot corrosion at 1000 °C for 20 h.

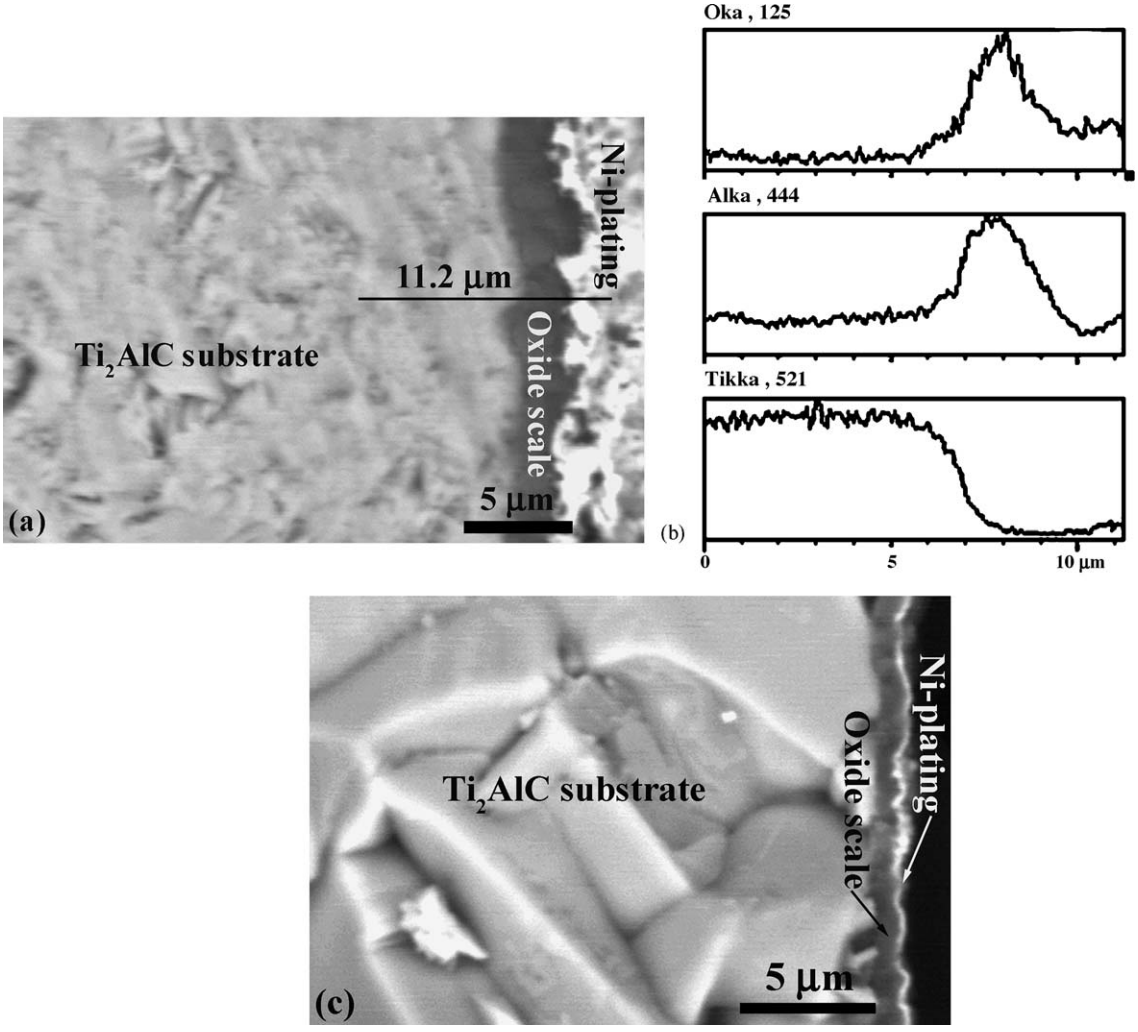

Fig. 9. Cross-sectional micrographs of the pre-oxidized samples. (a) Untreated; (b) EDS line-scanning result along the lines shown in (a); (c) after hot corrosion at 900 °C for 20 h.

We analyzed the corrosion products, surface and cross-sectional morphologies of the samples to understand the mechanism on improvement of corrosion resistance. XRD patterns of the pre-oxidized samples before and after hot corrosion tests are shown in Fig. 7. In all cases, Ti_2AlC is the predominant phase, implying that the corrosion scales are thin. Another feature is that the reflections of sodium–titanium oxides appear after corrosion tests and the intensities increase with temperature, while those of TiO_2 decreases as the temperature goes up to 1000 °C. It is clear that the reaction between TiO_2 and sodium sulfide occurred and TiO_2 is susceptible to molten salt. The reaction became more intense at 1000 °C, which accounts for the decrease of TiO_2 and increase of Na–Ti oxides. The amount of Al_2O_3 did not decrease apparently, suggesting that Al_2O_3 is much more resistant to hot corrosion against Na_2SO_4. The above results are supported by previous work reported by Lawson et al.[20]

Surface morphologies of the samples hot corroded at 900 and 1000 °C are similar and only the later is shown in Fig. 8. The corroded surface is relatively smooth and EDS analysis revealed that the products remained on the surface are mainly Al and O with minor amount of Ti and Na, which agrees well with the XRD results (Fig. 7). Cross-sectional analysis was also conducted to understand the improvement of corrosion-resistance. Fig. 9a displays the backscattered electron images of cross-sections of the sample pre-oxidized at 1000 °C for 2 h and the corresponding line-scanning result along the line shown in Fig. 9a is displayed in Fig. 9b. Combining the cross-sectional micrographs with line scan results, it is clear that a continuous Al_2O_3 scale formed after pre-oxidation treatment. Fig. 9c shows the fracture surface of the cross-section of the pre-oxidized sample after hot corrosion at 1000 °C for 20 h. It can be seen that the Al_2O_3 scale conserved after hot corrosion for 20 h and the scale is adherent to the Ti_2AlC substrate.

Unlike in the untreated sample, no sulfur-rich layer is present at the corrosion scale/substrate interface of the treated sample. The preformed Al_2O_3 scale efficiently prevented the reaction between Ti_2AlC and the molten salt. In other words, the presence of Al_2O_3 scale prevented the infiltration of Na_2SO_4 toward the corrosion scale/substrate interface. Furthermore, the difference on thermal expansion coefficients of the Ti_2AlC substrate ($9.0 \times 10^{-6}\,K^{-1}$) and that of Al_2O_3 ($8.8 \times 10^{-6}\,K^{-1}$ (parallel to *c*-axis) and $7.9 \times 10^{-6}\,K^{-1}$ (normal to *c*-axis)) is small in magnitude, which ensures low thermal stress and contributes to the stability of the Al_2O_3 scale on the Ti_2AlC substrate.[8]

Based on above analysis, it is evident that Ti_2AlC owes its improvement in corrosion resistance to the Al_2O_3 scale formed during the pre-oxidation treatment. The preformed Al_2O_3 scale is compatible with the Ti_2AlC substrate and can significantly improve the corrosion resistance of Ti_2AlC.

4. Conclusions

In conclusion, we investigated the hot corrosion behavior of Na_2SO_4-coated Ti_2AlC in air at 850–1000 °C. The hot corrosion kinetics is parabolic and protective Al_2O_3 scale retards the further corrosion of the Ti_2AlC substrate below the melting point of Na_2SO_4. Ti_2AlC suffers serious hot corrosion attacks at 900 and 1000 °C because porous and non-protective scales failed to protect the Ti_2AlC substrate. Chemical reactions between Ti_2AlC and the Na_2SO_4 salt dominate the corrosion process and sulfur segregated at the scale/substrate interfaces. A convenient and efficient pre-oxidation treatment can form a continuously protective Al_2O_3 scale, and consequently improve the hot corrosion resistance of Ti_2AlC by preventing the infiltration of Na_2SO_4 to the Ti_2AlC substrate.

Acknowledgements

This work was supported by the National Outstanding Young Scientist Foundation for Y. C. Zhou under Grant no. 59925208, Natural Sciences Foundation of China under no. 50232040, no. 50302011, and no. 90403027.

References

1. Jeitschko, W., Nowotny, H. and Benesovky, F., Kohlenstoffhaltige ternare verbindungen (H-phase). *Monatsh. Chem.*, 1963, **94**, 672.
2. Zhou, Y. C. and Sun, Z. M., Electronic structure and bonding properties of layered machinable Ti_2AlC and Ti_2AlN ceramic. *Phys. Rev. B*, 2000, **61**, 12570–12573.
3. Pietzka, M. A. and Schuster, J. C., Summary of constitutional data on the aluminium–carbon–titanium system. *J. Phase Equilib.*, 1994, **15**, 392–400.
4. Wang, X. H. and Zhou, Y. C., Solid–liquid reaction synthesis and simultaneous densification of polycrystalline Ti_2AlC. *Z. Metallkd.*, 2002, **93**, 66–71.
5. Lopacinski, M., Puszynski, J. and Lis, J., Synthesis of ternary titanium aluminum carbides using self-propagating high-temperature synthesis technique. *J. Am. Ceram. Soc.*, 2001, **84**, 3051–3053.
6. Barsoum, M. W., Ali, M. and El-Raghy, T., Processing and characterization of Ti_2AlC, Ti_2AlN and $TiAlC_{0.5}N_{0.5}$. *Metall. Mater. Trans. A*, 2000, **31**, 1857–1865.
7. Zhou, Y. C. and Wang, X. H., Deformation of polycrystalline Ti_2AlC under compression. *Mater. Res. Innovat.*, 2001, **5**, 87–93.
8. Wang, X. H. and Zhou, Y. C., High-temperature oxidation of Ti_2AlC in air. *Oxid. Met.*, 2003, **59**, 303–320.
9. Wang, J. Y. and Zhou, Y. C., Dependence of elastic stiffness on electronic band structure of nanolaminate M_2AlC (M = Ti, V, Nb, and Cr) ceramics. *Phys. Rev. B*, 2004, **69**, 214111.
10. Wilhelmsson, O., Palmquist, J. P., Nyberg, T. and Jansson, U., Deposition of Ti_2AlC and Ti_3AlC_2 epitaxial films by magnetron sputtering. *Appl. Phys. Lett.*, 2004, **85**, 1066–1068.
11. Wang, J. Y., Zhou, Y. C., Lin, Z. J., Meng, F. L. and Li, F., Raman active phonon modes and heat capacities of Ti_2AlC and Cr_2AlC ceramics: first-principles and experimental investigations. *Appl. Phys. Lett.*, 2005, **86**, 101902.
12. Spanier, J. E., Gupta, S., Amer, M. and Barsoum, M. W., Vibrational behavior of the $M_{n+1}AX_n$ phases from first-order Raman scattering (M = Ti, V, Cr, A = Si, X = C, N). *Phys. Rev. B*, 2005, **71**, 012103.
13. Lin, Z. J., Zhuo, M. J., Zhou, Y. C., Li, M. S. and Wang, J. Y., Microstructural characterization of layered-ternary Ti_2AlC. *Acta Mater.*, 2006, **54**, in press.
14. Brady, M. P. and Tortorelli, P. F., Alloy design of intermetallics for protective scale formation and for use as precursors for complex ceramic phase surfaces. *Intermetallics*, 2004, **12**, 779–789.
15. Yang, M. R. and Wu, S. K., The improvement of high-temperature oxidation of Ti–50Al by anodic coating in the phosphoric acid. *Acta Mater.*, 2002, **50**, 691–701.
16. Wang, X. H. and Zhou, Y. C., Oxidation behavior of Ti_3AlC_2 at 1000–1400 °C in air. *Corros. Sci.*, 2002, **45**, 891–907.

17. Kofstad, P., *High temperature corrosion*. Elsevier Applied Science, London and New York, 1988.
18. Wang, X. H. and Zhou, Y. C., Hot corrosion of Na_2SO_4-coated Ti_3AlC_2 in air at 700–1000 °C. *J. Electrochem. Soc.*, 2004, **151**, B505–B511.
19. Mobin, M. and Malik, A. U., Studies on the interactions of transition metal oxides and sodium sulfate in the temperature range 900–1200 K in oxygen. *J. Alloys Compd.*, 1996, **235**, 97–103.
20. Lawson, M. G., Pettit, F. S. and Blachere, J. R., Hot corrosion of alumina. *J. Mater. Res.*, 1993, **8**, 1964–1971.
21. Berthold, C. and Nickel, K. G., Hot-corrosion behaviour of silica and silica-formers: external versus internal control. *J. Eur. Ceram. Soc.*, 1998, **5**, 2365–2372.
22. Jacobson, N. S. and Smialek, J. L., Hot corrosion of sintered α-SiC at 1000 °C. *J. Am. Ceram. Soc.*, 1985, **68**, 432–439.
23. Kuranishi, T., Habazaki, H. and Konno, H., Oxidation-resistant multilayer coatings using an anodic alumina layer as a diffusion barrier on γ-TiAl substrates. *Surf. Coat. Technol.*, 2005, **200**, 2438–2444.
24. Lang, F. Q., Yu, Z. M., Gedevanishvili, S., Deevi, S. C. and Narita, T., Effect of pre-oxidation on the corrosion behavior of Fe–40Al sheet in a N_2–11.2O_2–7.5CO_2–500 ppm SO_2 atmosphere at 1273 K. *Intermetallics*, 2003, **11**, 129–134.
25. Mobin, M. and Malik, A. U., High-temperature interactions of transition-metal carbides with Na_2SO_4. *J. Less-Common Met.*, 1991, **170**, 243–254.